

## Title Page

Fluoxetine affects differentiation of midbrain dopaminergic neurons *in vitro*

Diana Lupu, Mukesh K. Varshney, Daniel Mucs, José Inzunza, Ulf Norinder, Felicia Loghin,  
Ivan Nalvarte, Joëlle Rüegg

Dept. of Toxicology, Iuliu Hațieganu University of Medicine and Pharmacy, Cluj-Napoca,  
Romania D.L.; F.L.

Dept. of Biosciences and Nutrition, Karolinska Institutet, Huddinge, Sweden M.K.V.; J.I.; I.N.

Unit of Work Environment Toxicology, Institute of Environmental Medicine, Karolinska  
Institutet, Stockholm, Sweden D.M.

Dept. Computer and Systems Sciences, Stockholm University, Kista, Sweden U.N.

Dept. of Clinical Neuroscience, Karolinska Institutet, Stockholm, Sweden J.R.

Swetox, Unit of Toxicology Sciences, Karolinska Institutet, Södertälje, Sweden D.L.; D.M.;  
U.N.; J.R.

## Running Title Page

Fluoxetine affects dopaminergic differentiation *in vitro*

Corresponding author:

Diana Lupu

Address: Pasteur street nr 6A, Cluj-Napoca, Romania

Mobile: +40 748 791 264.

E-mail address: lupu.diana@umfcluj.ro

Number of text pages: 31

Number of tables: 1

Number of figures: 10

Number of references: 53

Number of words in Abstract: 235

Number of words in Introduction: 750

Number of words in Discussion: 1399

ASD, Autism spectrum disorder; BERKO, Estrogen receptor  $\beta$  knock-out; DA, Dopaminergic; EDKB, Endocrine Disruptor Knowledge Base; En1, Homeobox engrailed-1; En2, Homeobox engrailed-2; ER, Estrogen receptor; FLX, Fluoxetine; Foxp2, Forkhead box protein P2; Gria2, Glutamate ionotropic receptor AMPA type subunit 2; Lmx1a, LIM Homeobox transcription factor 1 alpha; mDA, Midbrain dopaminergic; mDPC, Midbrain dopaminergic precursor cell; mESC, Mouse embryonic stem cell; Nes, Nestin; NPC; Neural precursor cell; Nkx2.2, NK2 homeobox 2; Otx2, Orthodenticle homeobox 2; Pax3, Paired box 3; Pitx3, Paired-like homeodomain transcription factor 3; Reln, Reelin; Rora, Retinoic acid receptor-related orphan receptor-alpha; SSRI, Selective serotonin reuptake inhibitor; Tubb3,  $\beta$ 3-tubulin; WT, Wild-type.

## Abstract

Recent meta-analyses found an association between prenatal exposure to the antidepressant fluoxetine (FLX) and an increased risk of autism in children. This developmental disorder has been related to dysfunctions in the brains' rewards circuitry, which, in turn, has been linked to dysfunctions in dopaminergic (DA) signalling. The present study investigated if FLX affects processes involved in dopaminergic neuronal differentiation. Mouse neuronal precursors were differentiated into midbrain dopaminergic precursor cells (mDPCs) and concomitantly exposed to clinically relevant doses of FLX. Subsequently, dopaminergic precursors were evaluated for expression of differentiation and stemness markers using qPCR. FLX treatment led to increases in early regional specification markers Orthodenticle homeobox 2 (*Otx2*) and Homeobox engrailed-1 and 2 (*En1* and *En2*). On the other hand, two transcription factors essential for midbrain dopaminergic (mDA) neurogenesis, LIM Homeobox transcription factor 1 alpha (*Lmx1a*) and Paired-like homeodomain transcription factor 3 (*Pitx3*) were down-regulated by FLX treatment. The stemness marker Nestin (*Nes*) was increased, whereas the neuronal differentiation marker  $\beta$ 3-tubulin (*Tubb3*) decreased. Additionally, we observed that FLX modulates the expression of several genes associated with ASD and down-regulates the estrogen receptors (ERs)  $\alpha$  and  $\beta$ . Further investigations using ER $\beta$  knock-out (BERKO) mDPCs showed that FLX had no or even opposite effects on several of the genes analyzed. These findings suggest that FLX affects differentiation of the dopaminergic system by increasing production of dopaminergic precursors, yet decreasing their maturation, partly via interference with the estrogen system.

## Introduction

FLX is the most commonly prescribed selective serotonin reuptake inhibitor (SSRI) and has been in clinical use since the late 1980s (Perez-Caballero et al., 2014). This highly lipophilic drug crosses the blood-brain barrier and selectively blocks the serotonin transporter in the brain, thus inhibiting serotonin reuptake from the synaptic cleft (Perez-Caballero et al., 2014). This leads to increased serotonergic neurotransmission resulting in antidepressant effects (Perez-Caballero et al., 2014). FLX is also widely prescribed to treat depression during pregnancy, despite a lack of knowledge regarding both treatment efficacy and risks for the foetus and child (Pei et al., 2016). Although FLX passes through the placental barrier, little is known about how it affects (neuro)developmental outcomes in children exposed *in utero* (Pei et al., 2016; Rampono et al., 2009).

Several studies have found an association between antenatal SSRI exposure and increased risks for autism spectrum disorders (ASD) in children. Three recent systematic reviews and meta-analyses of large case-control and cohort studies found associations between *in utero* SSRI exposure and an increased risk (1.5 to 2 fold) for ASD (Andalib et al., 2017; Kaplan et al., 2017; Man et al. 2015) and two others found associations between maternal use of antidepressants (including SSRIs) during pregnancy and increased risk for ASD in children (Mezzacappa et al., 2017; Rais et al., 2015). A number of rodent studies show reduced play behaviour and social motivation following perinatal administration of SSRIs (fluoxetine and citalopram), which is suggestive of neurodevelopmental disorders with impaired social behaviours, such as ASD (Khatri et al., 2014; Olivier et al., 2011; Rodriguez-Porcel et al., 2011; Simpson et al., 2011).

ASD is a neurodevelopmental disorder characterized by deficient social communication and interaction, as well as repetitive behavioural and activity patterns (American Psychiatric Association, 2013). The causes of ASD have not been fully elucidated, but the aetiology of this complex disorder is known to involve a combination of genetic and environmental factors that underlie dysfunctions in the amygdala, prefrontal cortex and nucleus accumbens (Chaste and Leboyer, 2012; Park et al., 2016). These brain areas are associated with social behaviour and social reward response, cognitive, language and emotion processing, all of which are deficient in autistic patients (Park et al., 2016). ASD is also linked only partially to hereditary components (about 50%) (Hallmayer et al., 2011), suggesting that environmental factors and toxicant exposure may play a more crucial role than initially considered (Varshney and Nalvarte 2017).

The social motivation hypothesis of autism was developed after observations of decreased motivation to attend to social stimuli in autistic children (Scott-Van Zeeland et al., 2010). This implies dysfunctions in the brains' reward circuitry, which, in turn, has been linked to dysfunctions in dopaminergic (DA) signaling (Dichter et al., 2012; Pavál, 2017; Scott-Van Zeeland et al., 2010). In mammals, the two main clusters of neurons that secrete dopamine are located in the midbrain and project to the nucleus accumbens, the prefrontal cortex and the caudate putamen (Dichter et al., 2012). The development of midbrain DA (mDA) neurons is orchestrated through the activity of transcription factors and morphogens that regulate midbrain patterning and specification of midbrain progenitor cells (Arenas et al., 2015).

To date there are no studies addressing the effects of prenatal FLX exposure on the mDA differentiation process as a possible source of abnormal DA neurotransmission during development. As mentioned above, mDA neurons are the main source of DA projections in the

mammalian brain and their early differentiation, in addition to maturation, could be critical for normal DA neurotransmission in the mesocorticolimbic and nigrostriatal pathways.

Mouse embryonic stem cells (mESC) offer a reliable and validated *in vitro* model for the assessment of prenatal toxicity of chemicals, including drugs (Bremer et. al., 2004). Recently, a well-defined mESC neural differentiation model (Lee et. al., 2000) has been successfully used to generate mDA neurons from mESCs *in vitro*, a process which was shown to be, to a certain extent, dependent on ER $\beta$  expression (Varshney et. al., 2017). For the present study, mDA neural precursors generated from mESCs were used to assess the effect of therapeutically relevant doses of FLX on the expression of key factors involved in midbrain fate specification. As this cell model lacks serotonergic synapses and considering previous evidence that FLX can affect estrogen receptor mRNA levels and transcriptional activity (Foran et al., 2004, Lister et al., 2009; Mennigen et al., 2008; Mennigen et al., 2010; Pop et al., 2015; Schultz et al., 2011), we also addressed the involvement of ERs in FLX's effects as a potential mode of action.

## **Materials and methods**

### ***Culture and maintenance of neural progenitor cells***

Wildtype (WT) and ER $\beta$ -knockout (BERKO) neural precursor cells (NPCs) were derived from mESCs as described earlier (Lee et. al., 2000, Varshney et al., 2017). NPCs were grown in neural expansion media containing Knockout DMEM/F-12 (without glutamine and HEPES, Life Technologies, Paisley, UK) supplemented with 1% N-2 Max (R&D systems, Abingdon, UK), 0.1% Gentamycin (from a 50 mg/mL solution, Life Technologies), 8.6 mM Glucose (Life Technologies), 0.5 mM L-glutamine (Life Technologies), 20 mM NaHCO<sub>3</sub> (Life Technologies), 10 ng/mL FGF basic (PeproTech, Rocky Hill, US) and 1  $\mu$ g/mL Laminin (Novus Biologicals, Abingdon, UK). NPCs were plated on Poly-L-Ornithine (50  $\mu$ g/mL, Sigma-Aldrich, Steinheim,

Germany) and Laminin (1  $\mu\text{g/mL}$ , Novus Biologicals) coated dishes at a seeding density of  $6 \times 10^4$  to  $1 \times 10^5$  cells/ $\text{cm}^2$ . Media was changed every day and cells were passaged at confluency using accutase (Life Technologies) for dissociation and spinning at 1500 rpm for 5 minutes.

### ***Differentiation of NPCs to midbrain precursor neurons***

NPCs (WT and BERKO) were differentiated to mDPCs by midbrain fate specification. In brief, NPCs were plated on Poly-L-ornithine (50  $\mu\text{g/mL}$ ) and Laminin (1  $\mu\text{g/mL}$ ) coated dishes at a seeding density of  $1.5\text{--}2 \times 10^5$  cells/ $\text{cm}^2$  in neural expansion media supplemented with Fibroblast Growth Factor basic (FGFb, 10 ng/mL, PeproTech), Fibroblast Growth Factor 8 basic (FGF8b, 100 ng/mL, Miltenyi Biotec GmbH, Teterow, Germany), Sonic hedgehog (Shh, 400 ng/mL, PeproTech) and Ascorbic acid (200  $\mu\text{M}$ , Tocris, Bristol, UK). The culture media was also supplemented with experimental doses of FLX at 1, 0.1 and 0.01  $\mu\text{M}$  (in DMSO) or DMSO at 0,1% (solvent control). Cells were maintained in this media for 6 days with a daily change of media. During this period NPCs generate midbrain precursor cells. On the 6<sup>th</sup> day media was removed, cells were washed with PBS and lysed with RLT Buffer (Qiagen, Hombrechtikon, Switzerland) supplemented with 1%  $\beta$ -mercaptoethanol.

### ***Quantitative Real-Time PCR (qPCR) analysis***

Total RNA was isolated from mDPCs using the AllPrep DNA/RNA Mini Kit and treated with DNase I (both from Qiagen). RNA concentrations were measured using a NanoQuant plate on Tecan Infinite M200 (Tecan, Männedorf, Switzerland) and RNA quality was checked with Bioanalyzer (Agilent technologies, Santa Clara, USA). 2000 ng RNA was used for reverse transcription with Superscript VILO cDNA Synthesis Kit (Life Technologies). qPCR was performed using 5 ng of cDNA, self-designed (Primer 3.0 web) exon-exon spanning primers (see Table 1) and KAPA SYBR Fast ABI Prism mastermix (Kapa Biosystems, Wilmington, USA), in

a 7500 RealTime PCR System (Applied Biosystems, Foster City, USA). PCR efficiency was calculated for each primer set using standard curves with serial dilutions of test samples. Primer efficiency was 2 in most of the sets used, representing the doubling in each cycle. Threshold cycle values for targets were determined in triplicates and P0 large ribosomal protein *Rplp0* (known as 36B4) was used as a reference gene. Relative fold changes compared to WT or BERKO controls were calculated using the Pfaffl or  $\Delta\Delta C_t$  method.

### ***Immunocytochemistry and fluorescence imaging***

Cells were grown on Poly-L-ornithine and Laminin coated chambered culture slides (Ibidi, Martinsried, Germany) and fixed in ice cold 4% paraformaldehyde (SantaCruz, Dallas, TX, USA) for 15 min followed by three washes (phosphate buffered saline, pH 7.4, PBS), incubated with blocking serum (1% bovine serum albumin (BSA) and 0.1% Tritonx-100 (both from Sigma-Aldrich) in PBS and stained with primary antibodies against Th (R&D Systems, Minneapolis, USA), En1 (Sigma-Aldrich), SERT (ThermoFisher, Waltham, USA) followed by detection with Alexa Fluor secondary antibodies (ThermoFisher) and DAPI (300 nM, Molecular Probes, Eugene, USA) with PBS washes between and after each incubation. Slides were observed under Axioplan2 epifluorescent microscope (Carl Zeiss, Oberkochen, Germany) using 20X objective (Fluor-Plan) with appropriate filter sets for each fluorophore and images were captured with Zeiss AxioCam MR scientific camera using Axiovision 4.0 software (Carl Zeiss). Appropriate negative and positive controls were incorporated for respective primary and secondary antibodies.

### ***Image analysis***

Quantification of immunoexpression density was performed by analyzing images in Fiji (ImageJ, NIH, Bethesda, USA) image analysis software using similar settings for each marker



across all images and experimental conditions. Neurite length measurements were performed on calibrated images using NeuronJ plugin in Fiji (Meijering et. al. 2004) with length threshold above 5  $\mu\text{m}$ .

### ***In silico ER binding predictions***

A molecular docking approach was used to detect potential interactions between FLX and the ERs. The X-ray structures of ER $\alpha$  and ER $\beta$  (Protein Data Bank ID: 1sj0 and 2fsz respectively) were acquired from the “A Database of Useful Decoys – Enhanced” [<http://dude.docking.org/>] database (Mysinger et al., 2012). A dataset of ER ligands containing 131 active and 101 inactive compounds was obtained from the U.S. Food and Drug Administration's Endocrine Disruptor Knowledge Base (EDKB) (Ding et al., 2010). The protein structures were prepared for docking using the Schrödinger Protein Preparation Wizard and the compounds from the EDKB ER dataset were prepared using the default settings of Schrödinger LigPrep. Docking simulations were performed using Schrödinger Glide (Friesner et al., 2004), with the default settings of the Glide SP (Single Precision) tool. The docking scores were then subsequently binned into 0.5 bins.

### ***Statistical analysis***

The experiments were performed three times with three technical replicates. If not stated otherwise, the statistical differences between groups were analyzed using the GraphPad Prism 6 software by one-way ANOVA, followed by Dunnett's test for multiple comparisons, or by Student's t-test for single comparisons. P-values < 0.05 were considered statistically significant unless stated otherwise. Data are shown as means  $\pm$  95% confidence intervals.

## **Results**

### ***FLX affects the differentiation of NPCs to midbrain precursors***

To assess if FLX affects early differentiation of the midbrain, we utilized a well-defined mESC model that mimics neural development *in vitro*, which is marked by the presence of early generating neural precursor cells (NPCs) and subsequent induction of midbrain dopaminergic precursor cells (mDPCs). Although immature, these mDPC cultures contain dopaminergic neuronal precursors that express tyrosine hydroxylase (*Th*) as well as low levels of the dopamine transporter (*Slc6a3*) (Figure 1A). However, these cells are nascent and do not form synapses yet. Using this cell model, we analysed the expression of genes that are critical for the early development of mDPCs, as well as mDA neurogenesis, following treatment with therapeutically relevant FLX concentrations. NPCs were differentiated to mDPCs by midbrain fate specification using a combination of FGFb, FGF8b, Shh and ascorbic acid. The cells were maintained for 6 days in culture medium with the induction cocktail and concomitantly exposed to a therapeutically relevant dose of FLX (0.1  $\mu$ M) or 0.1% DMSO (solvent control). Expression of *Th* was confirmed by immunocytochemistry (Figure 1B) in control and FLX treated cells and was higher in the FLX treated group ( $44.13 \pm 1.216$ ) compared to control ( $34.28 \pm 1.302$ ) (Figure 1A). However, the neuronal processes of *Th*<sup>+</sup> cells in the FLX treated group were smaller (mean neurite length ( $\mu$ m)  $11.72 \pm 0.5814$ ) (Figure 1C) and spindle shaped compared to well branched and longer processes in control group ( $19.37 \pm 0.6112$ ) (Figure 1B, magnified region of interest), suggesting that FLX interferes with the differentiation process of dopaminergic cells.

To investigate underlying transcriptional changes, mDPCs were treated with FLX (1, 0.1 or 0.01  $\mu$ M) and expression of genes critical for early regional specification and patterning of the ventral midbrain were measured. First, we analyzed the expression of the transcription factors Orthodenticle homeobox 2 (*Otx2*) and Homeobox engrailed-1 and 2 (*En1* and *En2*). FLX

treatment at 1 and 0.1  $\mu$ M increased mRNA expression of *Otx2* (1.24 and 1.21 mean fold change, respectively,  $p < 0.001$ , Figure 2A), of *En1* (1.17 and 1.19 fold change, respectively,  $p < 0.001$ , Figure 2C) and of *En2* (1.18 fold change,  $p = 0.015$  and 1.23 fold change,  $p = 0.0003$ , Figure 2D). In contrast, the expression of NK2 homeobox 2 (*Nkx2.2*), involved in midbrain fate determination and negatively regulated by *Otx2*, was down-regulated by FLX treatment at all tested concentrations ( $p < 0.0001$ , Figure 2B). Immunocytochemistry for *En1* confirmed its higher expression in mDPCs following FLX treatment ( $25.34 \pm 0.8686$ ) compared to solvent control ( $17.40 \pm 0.8201$ ,  $n = 12$ ) (Figure 2E).

We further analysed the expression of transcription factors essential for mDA neurogenesis, i.e. Paired-like homeodomain transcription factor 3 (*Pitx3*) and LIM Homeobox transcription factor 1 alpha (*Lmx1a*). FLX treatment at all concentrations, except 1  $\mu$ M FLX for *Lmx1a*, down-regulated expression of both *Pitx3* (0.89 fold change by 1  $\mu$ M FLX  $p = 0.0006$ ; 0.05 fold change by 0.1  $\mu$ M FLX,  $p < 0.001$  and 0.14 fold change by 0.01  $\mu$ M FLX,  $p < 0.001$  respectively) and *Lmx1a* (0.76 fold change by 0.1  $\mu$ M FLX,  $p = 0.0008$  and 0.58 fold change by 0.01  $\mu$ M FLX,  $p < 0.001$ ) (Figure 2G).

Next, we assessed if FLX affects stemness by analyzing the expression of the neural stem cell marker Nestin (*Nes*) and the neuronal marker  $\beta$ 3-tubulin (*Tubb3*) in mDPCs. We found that *Nes* expression was increased (Figure 3A) by FLX (1  $\mu$ M FLX caused a 1.35 fold change,  $p < 0.001$ ; FLX 0.1  $\mu$ M caused a 1.50 fold change,  $p < 0.001$  and FLX 0.01  $\mu$ M caused a 1.23 fold change,  $p = 0.0010$ ) and *Tubb3* (Figure 3B) was decreased by lower concentrations of FLX (0.1  $\mu$ M FLX induced a 0.79 fold change,  $p = 0.0028$  and 0.01  $\mu$ M FLX induced a 0.63 fold change,  $p < 0.0001$ ). Proper *Notch-Hes* signaling is essential for maintaining the neural progenitor identity and suppression of neuronal differentiation (Schuurmans & Guillemot, 2002). By analyzing the

expression of *Notch1* and its downstream effector *Hes1*, we observed a marked increase in the expression of both genes upon FLX treatment (*Notch1*: 2.40 fold change by 1  $\mu$ M FLX  $p<0.0001$ ; 1.67 fold change by 0.1  $\mu$ M FLX,  $p<0.0001$  and 1.43 fold change by 0.01  $\mu$ M FLX,  $p<0.05$ . *Hes1*: 5.38 fold change by 1  $\mu$ M FLX  $p<0.0001$ ; 2.51 fold change by 0.1  $\mu$ M FLX,  $p<0.001$  and 1.91 fold change by 0.01  $\mu$ M FLX,  $p<0.05$ .) (Figure 3C, D). These data suggest that FLX interferes with signaling cascades underlying precursor cell maintenance and maturation.

### ***FLX affects expression of genes associated with autism***

To evaluate if FLX modulates the expression of genes associated with ASD we measured the expression of forkhead box protein P2 (*Foxp2*), paired box 3 (*Pax3*), glutamate ionotropic receptor AMPA type subunit 2 (*Gria2*), retinoic acid receptor-related orphan receptor-alpha (*Rora*), and reelin (*Reln*), all of which not only play crucial roles in midbrain patterning and neurogenesis (Nguyen et al., 2010, Sarachana et al., 2011, Lammert & Howell 2006), but have also been implicated in autism (Bowers & Konopka 2012; Borg et al., 2002; Uzunova et al., 2014; Lammert & Howell et al., 2016; Nguyen et al., 2010). We observed a down-regulation of the expression of *Pax3* (0.41 fold change by 1  $\mu$ M FLX, 0.52 fold change by 0.1  $\mu$ M FLX,  $p<0.001$ ), *Rora* (0.60 fold change by 1  $\mu$ M FLX,  $p<0.05$ ; 0.61 fold change by 0.1  $\mu$ M FLX,  $p<0.05$  and 0.53 fold change by 0.01  $\mu$ M FLX,  $p<0.01$ ) and *Reln* (0.25 fold change by 1  $\mu$ M FLX,  $p<0.001$ ; 0.43 fold change by 0.1  $\mu$ M FLX,  $p<0.0001$  and 0.52 fold change by 0.01  $\mu$ M FLX,  $p<0.01$ ) (Figure 4). Additionally, increased levels of *En1* and *En2*, as shown in Figure 2 are also reported to correlate with ASD (James, et al., 2014; Kuemerle et al., 2007). These data suggest that FLX may indeed influence the expression of genes associated with ASD.

### ***FLX affects ER expression in midbrain precursors***

Since the mDPC cultures are too immature to form functioning synapses and any 5-HT produced is heavily diluted in the culture medium, the effect of FLX on the genes analysed in this study is likely not due to 5-HT reuptake inhibition. Increasing evidence points out to FLX having estrogen-disrupting effects (Foran et al., 2004; Lister et al., 2009; Lupu et al., 2017; Mennigen et al., 2008; Mennigen et al., 2010; Schultz et al., 2011), and in view of our recent data showing that ER $\beta$  plays an important role in the differentiation of midbrain dopaminergic neurons *in vitro* (by maintaining proper *Notch-Hes* signalling, among others) (Varshney et al., 2017), we addressed if treatment with this SSRI affects the expression levels of ERs in WT mDPCs, as well as if ER $\beta$  is involved in the observed effects of FLX by using ER $\beta$  knockout (BERKO) cells.

We observed that both ER $\alpha$  and ER $\beta$  are expressed in mDPCs (Figure 5A) and that ER $\alpha$  mRNA expression was down-regulated in both BERKO mDPCs (0.13 fold,  $p < 0.001$ ) and in WT mDPCs after FLX treatment compared to solvent control (0.24, 0.20 and 0.47 fold change by 1, 0.1 and 0.01  $\mu$ M FLX, respectively,  $p < 0.001$ , Figure 5B). Interestingly, in BERKO mDPCs, ER $\alpha$  levels were lower than in WT cells and FLX treatment did not reduce ER $\alpha$  expression any further compared to treatments in WT cells (Figure 5B). ER $\beta$  mRNA expression was also down-regulated in WT mDPCs after FLX treatment compared to solvent control (0.69, 0.22 and 0.39 fold change by 1, 0.1 and 0.01  $\mu$ M FLX, respectively,  $p < 0.001$ , Figure 5C).

### ***FLX effects on midbrain fate specification, but not maturation, are dependent on ER $\beta$***

To assess the role of ERs in mediating the effects of FLX on DA differentiation, we used BERKO NPCs to measure gene expression of the key factors analysed above. We observed that in BERKO mDPCs, FLX had no or even opposite effects on the genes involved in mDPC specification (*Otx2*, *Nkx2.2*, *En1*, and *En2*) (Figure 6) and the stemness marker *Nes* (Figure 7A),

suggesting that ERs are involved in the effects of FLX on early midbrain fate specification. In BERKO cells, *Otx2*, *En1*, *En2* and *Nes* mRNA expression was down-regulated after FLX treatment, as compared to BERKO solvent controls (Figure 6A, C, D and Figure 7A). Likewise, FLX treatment of BERKO mDPCs did not affect expression of the autism-related genes *Rora* or *Reln*, which was 3 fold and 15 fold decreased, respectively, in BERKO compared to WT mDPCs in control-treated cells (Figure 8).

On the other hand, in BERKO mDPCs FLX induced similar effects to those observed in WT mDPCs on the neuronal marker *Tubb3* (0.90 fold change by 0.1  $\mu$ M FLX,  $p=0.0104$ ; 0.80 fold change by 0.01  $\mu$ M FLX,  $p<0.0001$ , Figure 7B) and on the neurogenesis factors *Pitx3* (0.50, 0.12 and 0.12 fold change by 1, 0.1 and 0.01  $\mu$ M FLX, respectively,  $p<0.001$ ) and *Lmx1a* (0.75 fold change,  $p=0.001$  for FLX 0.1  $\mu$ M; 0.53 fold change,  $p<0.001$  for FLX 0.01  $\mu$ M), decreasing their mRNA expression compared to BERKO solvent controls (Figure 7C, D).

### ***FLX is a potential ER binder***

As our results indicate the involvement of ERs in mediating some of the effects of FLX, we investigated if FLX could bind these receptors using molecular docking predictions. The results showed that both ER $\alpha$  and ER $\beta$  can bind FLX through a combination of hydrophobic and polar interactions (Figure 9A, B). Hydrophobic interactions within ER ligand binding pockets (LBPs) were mainly mediated by leucine/isoleucine (Leu/Ile) and phenylalanine (Phe) amino acid residues, whereas hydrogen bonds could form between the secondary amino group present in FLX and glutamate (Glu353/Glu42) residues in ER LBPs. The low docking energies, located in the -9.0 to -8.5 bin for both ER $\alpha$  and ER $\beta$  (Figure 10A, B), suggest that FLX has a fairly strong tendency to bind to ERs. The probabilities for binding of FLX to ER $\alpha$  and ER $\beta$  are 0.88 and 0.74, respectively.

## Discussion

To address prenatal FLX effects on the early differentiation of mDA fate from neural precursors, we employed a well-defined and highly controlled mESC cell model which reflects many of the key aspects of midbrain stem cell fate acquisition and development (Lee et al., 2000; Varshney et al., 2017). *In vivo*, the development of midbrain dopaminergic neurons begins with the patterning of the neural tube and is orchestrated by the isthmus organizer and the floor plate (Arenas et al., 2015). The isthmus organizer is located at the midbrain-hindbrain boundary and is represented by a group of cells with a complex pattern of gene expression that includes the signaling factors FGF8 (fibroblast growth factor 8) and *Wnt1* (wingless-int1) and transcription factors *Otx2*, *Gbx2* (gastrulation brain homeobox 2), *Pax2* (paired box 2) and *En1/2*, among others (Arenas et al., 2015). The midbrain floor plate is a glial structure located along the ventral midline of the neural tube and modulates cell identity in the dorsal-ventral position by secreting the morphogens Shh and Wnt1 (Arenas et al., 2015). Thus, the coordinated activity of these transcription factors and morphogens regulates ventral midbrain patterning and the specification of ventral midbrain progenitor cells. Besides ventralization, the midbrain floor plate has neurogenic potential and is the source of dopaminergic precursors, subsequently giving rise to dopaminergic neurons (Hegarty et al., 2013). *In vitro*, mature midbrain dopaminergic neurons (mDNs) have been successfully generated from mESCs, using highly controlled culture conditions to guide the differentiation process toward NPCs and, subsequently, to mDPCs and mDNs (Varshney et al., 2017). The mDNs obtained from both WT and BERKO mDPCs express the dopaminergic markers *Th* (tyrosine hydroxylase, the enzyme which catalyzes the rate limiting step of catecholamine synthesis) and *Slc6a3* (Solute Carrier Family 6 Member 3, the

presynaptic dopamine transporter) and have functional dopamine synthesis and release (Varshney et al., 2017).

Our results show that FLX exposure, in therapeutically relevant doses, affects the differentiation process from NPCs to mDPCs. To our knowledge, there are no data on FLX kinetics in the fetus and FLX levels in the fetal brain. Thus we chose therapeutically relevant FLX concentrations (0.01, 0.1 and 1  $\mu$ M) as infant cord blood and plasma concentrations reported in the literature, which are in the range of 0.037 to 1.06  $\mu$ M (Heikkinen et al., 2002; Kim et al., 2006; Gurnot et al., 2015).

We found that FLX up-regulates transcription factors *Otx2*, *En1* and *En2*, which are essential for ventral midbrain patterning, while *Nkx2.2* was down-regulated. *Otx2*, *En1* and *En2*, among others, are expressed as early as embryonic day 7-8 (E7-8) in the mouse and are critical for the formation and positioning of the isthmus organizer, thus contributing to the patterning and determination of midbrain precursors (Arenas et al., 2015; Hegarty et al., 2013). *Otx2* is also essential for the neurogenic potential of the floor plate (Hegarty et al., 2013). Conversely, *Nkx2.2* is a negative regulator of midbrain dopaminergic development and is repressed by *Otx2* (Abeliovich and Hammond, 2007). A lower expression of *Nkx2.2* favours dopaminergic neuron differentiation at the expense of serotonergic neurons (Abeliovich and Hammond, 2007). Thus our results suggest that FLX increases differentiation of NPCs to midbrain precursors, which might lead to a decrease in serotonergic neurons.

On the other hand, we observed that the expression of the mDA markers *Lmx1a* and *Pitx3* were down-regulated upon FLX treatment. *Lmx1a* is induced by *Otx2* and is required for the specification of mDA neurons and suppression of alternative fates (Arenas et al., 2015; Hegarty et al., 2013). *Pitx3* is part of a network of transcription factors that cooperate to induce mDA



neurogenesis and is also important for mDA neuronal survival (Hegarty et al., 2013). Concomitantly, the stemness marker *Nes* was up-regulated, while the neuronal differentiation marker *Tubb3* was down-regulated. Interestingly, the mRNA expression of *Pitx3*, *Lmx1a* and *Tubb3* was lower after treatment with submicromolar FLX, suggesting that at 1  $\mu$ M, FLX may be interacting with targets that compensate the down-regulation of these neurogenesis markers. *Th* expression was increased following submicromolar FLX (0.1  $\mu$ M) however, the nascent *Th* positive cells in this group had spindle shaped morphology compared to more branched processes in untreated mDPCs. This could be due to feedback mechanisms during which cells produce more enzyme to synthesize dopamine while the progenitors still cannot mature due to aberrant signaling and expression of other factors such as reelin. Together, these findings suggest that although FLX promotes mDA fate determination, it prevents the midbrain precursors to progress into mature DA neurons.

These effects on dopaminergic differentiation might contribute to the association between developmental FLX exposure and increased risk for ASD. Importantly, some of the genes that we have found dysregulated by FLX are known to be associated with ASD (*En1/2*, *Pax3*, *Rora*, and *Reln*). *En2* has been associated with ASD in genetic linkage studies and increased *En2* gene expression and protein levels were detected in the cerebellum of autistic subjects (Kuemerle et al., 2007; James et al., 2014). A study on postmortem brain tissue revealed decreased *Rora* protein levels in the cerebellum and frontal cortex of autistic individuals, which was consistent with increased CpG methylation in the upstream promoter region of *Rora* (Nguyen et al., 2010). Similarly, decreased *Reln* mRNA and protein was observed in the cerebellum and superior frontal cortex of autistic subjects (Lammert & Howell et al., 2016). *Reln* is critical for proper cell positioning and neuronal migration during development, and increasing evidence suggests that

heterozygous mutations in *Reln*, including *de novo* mutations, contribute to the autistic phenotype (Lammert & Howell et al., 2016). Finally, a cryptic deletion including part of the *Pax3* gene and a *de novo* translocation were observed in an ASD patient (Borg et al., 2002)

Several studies suggest that FLX affects estrogenic signaling in fish and mammals (Foran et al., 2004; Lister et al., 2009; Lupu et al., 2017; Mennigen et al., 2008; Mennigen et al., 2010; Schultz et al., 2011) and FLX has been shown to modulate ER transcriptional activation at (sub)micromolar concentrations using a reporter gene assay in breast cancer cells expressing both ERs (Pop et al., 2015). Proper estrogenic signaling is essential for normal brain development, influencing apoptosis, synaptogenesis and neuronal morphometry (McCarthy, 2008). In a recent study, we have shown that ER $\beta$  facilitates midbrain dopaminergic fate and function largely ligand-independently (Varshney et al., 2017) and that loss of ER $\beta$  had similar effects on DA differentiation as we observe here with FLX treatment. Furthermore, ligand-mediated effects have also been shown as NPCs treated with estradiol during differentiation to mDPCs *in vitro* resulted in an increased proliferation of mDPCs expressing *Lmx1a* and in a higher proportion of dopaminergic neurons (Diaz et al., 2009). Estradiol action was mediated through nuclear ERs, as ICI182780 (ER antagonist) abolished the effect on proliferation of committed precursors and subsequent differentiation (Diaz et al., 2009). In our study, we showed that FLX decreases ER $\alpha$  and ER $\beta$  levels and that its effects on dopaminergic differentiation are abolished or even counteracted in BERKO cells, with the exception of *Tubb3*, *Lmx1a* and *Pitx3* down-regulation. Notably, ER $\alpha$  is also strongly decreased in the BERKO cells and we show that FLX is predicted to bind to both ERs *in silico*, suggesting an involvement of one or both of these receptors in the observed effects. Nevertheless mDPCs do not form synapses, and although they express the serotonin transporter *Slc6a4* (Supplementary Figure 1A, B), only low *Tph2* levels are

detected in these cells (Supplementary Figure 1A), and any 5-HT produced is greatly diluted in the medium. Therefore, the effect of FLX in our mDPC model is likely not mediated through 5-HT reuptake inhibition, rather by its modulation of other factors, such as the ERs. Hence our study suggests that the roles of the ER isoforms upon FLX administration should be further investigated.

For some of the genes examined (e.g. *Pitx3*, *Nes*, *ER $\alpha$* , *ER $\beta$* ), we observed a non-monotonic dose-response (defined as a nonlinear relationship between dose and effect where the slope of the curve changes sign within the range of doses examined) and for other genes (e.g. *Nkx2.2*, *Lmx1a*, *Tubb3*) the effect size was greater at lower concentrations (in the nanomolar range) (Vandenberg et al., 2012). Both nonmonotonic and low-dose responses have been previously observed for chemicals that act on targets involved in endocrine regulation (including the ERs) and there is extensive literature from *in vitro*, *in vivo* and epidemiological studies in support of these concepts (Vandenberg et al., 2012).

## **Conclusion**

In conclusion, we show here that FLX affects differentiation of dopaminergic neurons, possibly by interfering with the nuclear ERs. Our findings suggest that FLX increases neural specification towards the dopaminergic phenotype, yet decreases dopaminergic neurogenesis. This calls for further studies to establish if these molecular events are linked to the development of the dopaminergic system in humans and to address their involvement in the association between prenatal FLX exposure and increased ASD risk in children.

## **Authorship Contributions**

*Participated in research design:* Lupu, Varshney, Nalvarte, Inzunza, Rüegg

*Conducted experiments:* Lupu, Varshney, Nalvarte, Norinder, Mucs

*Contributed new reagents or analytic tools:* Nalvarte, Inzunza

*Performed data analysis:* Lupu, Varshney, Nalvarte, Norinder, Mucs

*Wrote or contributed to the writing of the manuscript:* Lupu, Varshney, Nalvarte, Inzunza,  
Norinder, Mucs, Loghin, Rüegg

## References

Abeliovich A and Hammond R (2007) Midbrain dopamine neuron differentiation: factors and fates. *Dev Biol* **304**: 447-54.

American Psychiatric Association (2013) Autism Spectrum Disorder, in Diagnostic and Statistical Manual of Mental Disorders, Fifth Edition, pp 50-59, American Psychiatric Association, Arlington, VA.

Andalib S, Emamhadi M, Yousefzadeh-Chabok S, Shakouri SK, Høilund-Carlsen PF, Vafaei MS Sheldrick-Michel TM (2017) Maternal SSRI exposure increases the risk of autistic offspring: A meta-analysis and systematic review. *Eur Psychiatry* **45**:161-166.

Arenas E, Denham M, Villaescusa JC (2015) How to make a midbrain dopaminergic neuron. *Development* **142**: 1918-1936.

Borg I, Squire M, Menzel C, Stout K, Morgan D, Willatt L, O'Brien PC, Ferguson-Smith MA, Ropers HH, Tommerup N, Kalscheuer VM, Sargan DR (2002) A cryptic deletion of 2q35 including part of the PAX3 gene detected by breakpoint mapping in a child with autism and a de novo 2;8 translocation. *J Med Genet* **39**:391-399.

Bowers JM, Konopka G (2012) The role of the FOXP family of transcription factors in ASD. *Dis Markers* **33**:251-260.

Bremer S, Hartung T (2004) The use of embryonic stem cells for regulatory developmental toxicity testing in vitro-the current status of test development. *Curr Pharm Des* **10**: 2733-2747.

Chaste P and Leboyer M (2012) Autism risk factors: genes, environment, and gene-environment interactions. *Dialogues Clin Neurosci* **14**: 281-292.

Díaz NF, Díaz-Martínez NE, Camacho-Arroyo I, Velasco I (2009) Estradiol promotes proliferation of dopaminergic precursors resulting in a higher proportion of dopamine neurons derived from mouse embryonic stem cells. *Int J Dev Neurosci* **27**:493-500.

Dichter GS, Damiano CA, Allen JA (2012) Reward circuitry dysfunction in psychiatric and neurodevelopmental disorders and genetic syndromes: animal models and clinical findings. *J Neurodev Disord* **4**: 19.

Ding D, Xu L, Fang H, Hong H, Perkins R, Harris S, Bearden ED, Shi L, Tong W (2010) The EDKB: an established knowledge base for endocrine disrupting chemicals. *BMC Bioinformatics* **11**:S5.

Foran CM, Weston J, Slattery M, Brooks BW, Huggett DB (2004) Reproductive assessment of Japanese medaka (*Oryzias latipes*) following a four-week fluoxetine (SSRI) exposure. *Arch Environ Contam Toxicol* **46**: 511-517.

Friesner RA, Banks JL, Murphy RB, Halgren TA, Klicic JJ, Mainz DT, Repasky MP, Knoll EH, Shelley M, Perry JK, Shaw DE, Francis P, Shenkin PS (2004) Glide: a new approach for rapid, accurate docking and scoring. 1. Method and assessment of docking accuracy. *J Med Chem* **47**:1739-1749.

Gurnot C, Martin-Subero I, Mah SM, Weikum W, Goodman SJ, Brain U, Werker JF, Kobor MS, Esteller M, Oberlander TF, Hensch TK (2015) Prenatal antidepressant exposure associated with CYP2E1 DNA methylation change in neonates. *Epigenetics* **10**:361–372.

Hallmayer JI, Cleveland S, Torres A, Phillips J, Cohen B, Torigoe T, Miller J, Fedele A, Collins J, Smith K, Lotspeich L, Croen LA, Ozonoff S, Lajonchere C, Grether JK, Risch N (2011) Genetic heritability and shared environmental factors among twin pairs with autism. *Arch Gen Psychiatry* **68**: 1095-1102.

Hegarty SV, Sullivan AM, O'Keeffe GW (2013) Midbrain dopaminergic neurons: a review of the molecular circuitry that regulates their development. *Dev Biol* **379**:123-138.

Heikkinen T, Ekblad U, Palo P, Laine K (2003) Pharmacokinetics of fluoxetine and norfluoxetine in pregnancy and lactation. *Clin Pharmacol Ther* **73**:330-337.

Hu VW, Sarachana T, Sherrard RM, Kocher KM (2015) Investigation of sex differences in the expression of RORA and its transcriptional targets in the brain as a potential contributor to the sex bias in autism. *Mol Autism* **6**:7.

James SJ, Shpyleva S, Melnyk S, Pavliv O, Pogribny IP (2014) Elevated 5-hydroxymethylcytosine in the Engrailed-2 (EN-2) promoter is associated with increased gene expression and decreased MeCP2 binding in autism cerebellum. *Transl Psychiatry*, **4**:e460.

Kaplan YC, Keskin-Arslan E, Acar S, Sozmen K (2017) Maternal SSRI discontinuation, use, psychiatric disorder and the risk of autism in children: a meta-analysis of cohort studies. *Br J Clin Pharmacol* **83**: 2798-2806.

Khatri N, Simpson KL, Lin RCS, Paul IA (2014) Lasting Neurobehavioral Abnormalities in Rats After Neonatal Activation of Serotonin 1A and 1B Receptors: Possible Mechanisms for Serotonin Dysfunction in Autistic Spectrum Disorders. *Psychopharmacology (Berl)* **231**: 1191–1200.

Kim J, Riggs KW, Misri S, Kim J, Riggs KW, Misri S, Kent N, Oberlander TF, Grunau RE, Fitzgerald C, Rurak DW (2006) Stereoselective disposition of fluoxetine and norfluoxetine during pregnancy and breast-feeding. *Br J Clin Pharmacol* **61**:155–163.

Kuemerle B, Gulden F, Cherosky N, Williams E, Herrup K (2007) The mouse Engrailed genes: a window into Autism. *Behav brain res* **176**:121-132.

Lammert DB, Howell BW (2016) RELN Mutations in Autism Spectrum Disorder. *Front Cell Neurosci* **10**:84.

Lee SH, Lumelsky N, Studer L, Auerbach JM, McKay RD (2000). Efficient generation of midbrain and hindbrain neurons from mouse embryonic stem cells. *Nat Biotechnol* **18**: 675-679.

Lister A, Regan C, Van Zwol J, Van Der Kraak G (2009) Inhibition of egg production in zebrafish by fluoxetine and municipal effluents: a mechanistic evaluation. *Aquat Toxicol* **95**: 320-329.

Lupu D, Sjödin MOD, Varshney M, Lindberg J, Loghin F, Rüegg J (2017) Fluoxetine modulates sex steroid levels in vitro. *Clujul Med* **90**: 420–424.

Man KK, Tong HH, Wong LY, Chan EW, Simonoff E, Wong IC (2015) Exposure to selective serotonin reuptake inhibitors during pregnancy and risk of autism spectrum disorder in children: a systematic review and meta-analysis of observational studies. *Neurosci Biobehav Rev* **49**: 82-89.

McCarthy MM (2008) Estradiol and the developing brain. *Physiol Rev* **88**: 91-124.

Meijering E, Jacob M, Sarria JC, Steiner P, Hirling H, Unser M (2004) Design and validation of a tool for neurite tracing and analysis in fluorescence microscopy images. *Cytometry A* **58**:167-176.

Mennigen JA, Martyniuk CJ, Crump K, Xiong H, Zhao E, Popesku J, Anisman H, Cossins AR, Xia X, Trudeau VL (2008) Effects of fluoxetine on the reproductive axis of female goldfish (*Carassius auratus*). *Physiol Genomics*. **35**: 273-282.

Mennigen JA, Lado WE, Zamora JM, Duarte-Guterman P, Langlois VS, Metcalfe CD, Chang JP (2010) Waterborne fluoxetine disrupts the reproductive axis in sexually mature male goldfish, *Carassius auratus*. *Aquat Toxicol* **100**: 354-364.



Mezzacappa A, Lasica PA, Gianfagna F, Cazas O, Hardy P, Falissard B, Sutter-Dallay AL, Gressier F (2017) Risk for Autism Spectrum Disorders According to Period of Prenatal Antidepressant Exposure: A Systematic Review and Meta-analysis. *JAMA Pediatr* **171**: 555-563.

Mysinger MM, Carchia M, Irwin JJ, Shoichet BK (2012) Directory of useful decoys, enhanced (DUD-E): better ligands and decoys for better benchmarking. *J Med Chem* **55**:6582-6594.

Nguyen A, Rauch TA, Pfeifer GP, Hu VW (2010) Global methylation profiling of lymphoblastoid cell lines reveals epigenetic contributions to autism spectrum disorders and a novel autism candidate gene, RORA, whose protein product is reduced in autistic brain. *FASEB J* **24**:3036-3051.

Olivier JDA, Vallès A, van Heesch F, Afrasiab-Middelmann A, Roelofs JJPM, Jonkers M, Peeters EJ, Korte-Bouws GAH, Dederen JP, Kiliaan AJ, Martens GJ, Schubert D, Homberg JR (2011) Fluoxetine administration to pregnant rats increases anxiety-related behavior in the offspring. *Psychopharmacology (Berl)* **217**: 419–432.

Park HR, Lee JM, Moon HE, Lee DS, Kim B-N, Kim J, Kim DG, Paek SH (2016) A Short Review on the Current Understanding of Autism Spectrum Disorders. *Exp Neurobiol* **25**: 1-13.

Pavál D (2017) A Dopamine Hypothesis of Autism Spectrum Disorder. *Dev Neurosci* **39**: 355-360.

Pei S, Liu L, Zhong Z, Wang H, Lin S, Shang J (2016) Risk of prenatal depression and stress treatment: alteration on serotonin system of offspring through exposure to Fluoxetine. *Sci Rep* **6**: 33822.

Perez-Caballero L, Torres-Sanchez S, Bravo L, Mico JA, Berrocoso E (2014) Fluoxetine: a case history of its discovery and preclinical development. *Expert Opin Drug Discov* **9**: 567-578.

Pop A, Lupu DI, Cherfan J, Kiss B, Loghin F (2015) Estrogenic/antiestrogenic activity of selected selective serotonin reuptake inhibitors. *Clujul Med* **88**: 381-385.

Rais TB, Rais A (2014) Association Between Antidepressants Use During Pregnancy and Autistic Spectrum Disorders: A Meta-analysis. *Innov Clin Neurosci* **11**: 18–22.

Rampono J, Simmer K, Ilett KF, Hackett LP, Doherty DA, Elliot R, Kok CH, Coenen A, Forman T (2009) Placental transfer of SSRI and SNRI antidepressants and effects on the neonate. *Pharmacopsychiatry* **42**: 95-100.

Rodriguez-Porcel F, Green D, Khatri N, Harris SS, May WL, Lin RCS, Paul IA (2011) Neonatal Exposure of Rats to Antidepressants Affects Behavioral Reactions to Novelty and Social Interactions in a Manner Analogous to Autistic Spectrum Disorders. *Anat rec (Hoboken)* **294**: 1726-1735.

Sarachana T, Xu M, Wu RC, Hu VW (2011) Sex hormones in autism: androgens and estrogens differentially and reciprocally regulate RORA, a novel candidate gene for autism. *PLoS One* **6**:e17116.

Schultz MM, Painter MM, Bartell SE, Logue A, Furlong ET, Werner SL, Schoenfuss HL (2011) Selective uptake and biological consequences of environmentally relevant antidepressant pharmaceutical exposures on male fathead minnows. *Aquat Toxicol* **104**: 38-47.

Schuermans C, Guillemot F (2002) Molecular mechanisms underlying cell fate specification in the developing telencephalon. *Curr Opin Neurobiol* **12**:26-34.

Scott-Van Zeeland AA, Dapretto M, Ghahremani DG, Poldrack RA, Bookheimer SY (2010) Reward Processing in Autism. *Autism res* **3**: 53-67.

Simpson KL, Weaver KJ, de Villiers-Sidani E, Lu JY-F, Cai Z, Pang Y, Rodriguez-Porcel F, Paul IA, Merzenich M, Lin RCS (2011) Perinatal antidepressant exposure alters cortical network function in rodents. *Proc Natl Acad Sci USA* **108**: 18465-18470.

Uzunova G, Hollander E, Shepherd J (2014) The role of ionotropic glutamate receptors in childhood neurodevelopmental disorders: autism spectrum disorders and fragile x syndrome. *Curr Neuropsychopharmacol* **12**:71-98.

Vandenberg LN, Colborn T, Hayes TB, Heindel JJ, Jacobs DR Jr, Lee DH, Shioda T, Soto AM, vom Saal FS, Welshons WV, Zoeller RT, Myers JP. Hormones and endocrine-disrupting chemicals: low-dose effects and nonmonotonic dose responses. *Endocr Rev* **33**:378-455.

Varshney M and Nalvarte I (2017) Genes, Gender, Environment, and Novel Functions of Estrogen Receptor Beta in the Susceptibility to Neurodevelopmental Disorders. *Brain Sci* **7**: pii: E24.

Varshney MK, Inzunza J, Lupu D, Ganapathya V, Antonson P, Rüegg J, Nalvarte I, Gustafsson J-Å (2017) Role of estrogen receptor beta in neural differentiation of mouse embryonic stem cells. *Proc Natl Acad Sci USA* **114**: E10428–E10437.

## Footnotes

This work was supported by the Swedish Research Council Formas [Grants 210-2012-1502, 216-2013-1966]; and by Emil & Wera Cornell's research foundation. \*Diana Lupu, Mukesh K. Varshney, Ivan Nalvarte and Joëlle Rüegg contributed equally

## Legends for figures

**Fig. 1. Dopaminergic marker expression in mDPCs.** (A) *Th* and *Slc6a3* mRNA expression relative to *Rplp0* expression in mDPCs treated with solvent (CTRL) or with 0.1  $\mu$ M FLX for 6 days. (B) Representative images of Th immunoreactivity in mDPCs upon control (CTRL) or 0.1  $\mu$ M FLX treatments. Right panels represent quantifications (mean gray value). Enlarged yellow box insets in (B) represent spindle shaped (in 0.1  $\mu$ M FLX) and normally branched Th positive cells (in CTRL) and (C) Neurite length measurements of Th positive cells in control (CTRL) or 0.1  $\mu$ M FLX treated mDPCs. Data represent means  $\pm$  CI from 3 independent experiments in triplicates. Significant differences (two-way ANOVA for A; t-test for B and C) as compared to control are marked with asterisks (\*\* for  $p < 0.01$ , \*\*\* for  $p < 0.001$ ). Scale bar: 100  $\mu$ m in B.

**Fig.2. FLX affects factors essential for midbrain patterning, specification and mDA neurogenesis.** WT NPCs were differentiated into mDPCs and concomitantly treated with 1, 0.1, and 0.01  $\mu$ M FLX. Subsequently, mRNA expression of *Otx2* (A), *Nkx2.2* (B), *En1* (C), and *En2* (D) was measured using qPCR. (E) Representative images of immunohistochemistry of En1 in control and FLX treated midbrain precursors. Right panel represents quantification (mean gray value) of (E). (F) Expression of *Pitx3* and (G) *Lmx1a* upon control FLX treatments.. Data represent means  $\pm$ CI from 3 independent experiments in triplicates. Significant differences (one-way ANOVA, A, B, C, D, F, G, and t-test, E) as compared to control are marked with asterisks (\*\* for  $p < 0.01$ ; \*\*\* for  $p < 0.001$ ). Scale bar: 100  $\mu$ m in (E).

**Fig.3. FLX affects factors of neural stemness and differentiation markers in mDPCs.** WT NPCs were differentiated into mDPCs and concomitantly treated with 1, 0.1, and 0.01  $\mu$ M FLX. Subsequently, mRNA expression of *Nes* (A), *Tubb3* (B), *Notch1* (C) and *Hes1* (D) was measured

using qPCR. Data represent means  $\pm$ CI from 3 independent experiments in triplicates. Significant differences (one-way ANOVA) as compared to control are marked with asterisks (\* for  $p < 0.05$ ; \*\* for  $p < 0.01$ ; \*\*\* for  $p < 0.001$ ).

**Fig.4. FLX treatment of mDPCs affects some genes associated with autism.** Relative change in mRNA expression levels of (A) *Foxp2*, (B) *Pax3*, (C) *Gria2*, (D) *Rora*, and (E) *Reln* for control (CTRL) or 1, 0.1, and 0.01  $\mu$ M FLX treatments in mDPCs. Data represent means  $\pm$ CI from 3 independent experiments in triplicates. Significant differences (one-way ANOVA) as compared to WT control treated cells are marked with asterisks (\* for  $p < 0.05$ ; \*\* for  $p < 0.01$ ; \*\*\* for  $p < 0.001$ ).

**Fig.5. FLX affects ER $\alpha$  and ER $\beta$  expression in mDPCs.** WT and BERKO NPCs were differentiated into mDPCs and concomitantly treated with 1, 0.1, and 0.01  $\mu$ M FLX. (A) mRNA expression of ER $\alpha$  and ER $\beta$  relative to *Rplp0* in WT and BERKO mDPCs, (B) fold change in mRNA expression of ER $\alpha$  in WT and BERKO mDPCs and (C) ER $\beta$  in WT mDPCS following FLX treatments. Data represent means  $\pm$ CI from 3 independent experiments in triplicates. Significant differences (one-way ANOVA) as compared to WT CTRL are marked with asterisks (\*\*\* for  $p < 0.001$ ).

**Fig.6. Loss of ER $\beta$  attenuates the FLX-mediated effects on factors essential for midbrain patterning and mDPC specification.** BERKO NPCs were differentiated into mDPCs and concomitantly treated with 1, 0.1, and 0.01  $\mu$ M FLX. Subsequently, mRNA expression of *Otx2* (A), *Nkx2.2* (B), *En1* (C), and *En2* (D) was measured using qPCR. Data represent means  $\pm$ CI from 3 independent experiments in triplicates. Significant differences (one-way ANOVA) are marked with asterisks (\* for  $p < 0.05$ ; \*\* for  $p < 0.01$ ; \*\*\* for  $p < 0.001$ )

**Fig.7. FLX affects factors of neural stemness and mDA neurogenesis in mDPCs.** BERKO

NPCs were differentiated into mDPCs and concomitantly treated with 1, 0.1, and 0.01  $\mu$ M FLX. Subsequently, mRNA expression of (A) *Nes*, (B) *Tubb3*, (C) *Pitx3*, and (D) *Lmx1a* was measured using qPCR. Data represent means  $\pm$ CI from 3 independent experiments in triplicates. Significant differences (one-way ANOVA) are marked with asterisks (\* for  $p < 0.05$ , \*\* for  $p < 0.01$ ; \*\*\* for  $p < 0.001$ ).

**Fig.8. FLX affects ASD-associated genes important for neuronal development.** WT and BERKO

NPCs were differentiated into mDPCs and concomitantly treated with 1, 0.1, and 0.01  $\mu$ M FLX. Subsequently, mRNA expression of *Rora* (A) and *Reln* (B) was measured using qPCR. Data represent means  $\pm$ CI from 3 independent experiments in triplicates. Significant differences (two-way ANOVA, followed by Turkey's test) are marked with asterisks (\* for  $p < 0.05$ ; \*\*\* for  $p < 0.001$ ; ns, no significance).

**Fig.9. FLX in ER $\alpha$  (A) and ER $\beta$  (B) binding pocket represented via the Schrödinger Ligand**

Interaction Diagram

**Fig.10. Docking scores of ER $\alpha$  (A) and ER $\beta$  (B) with known active (light grey) and inactive (black) compounds in relation to FLX (dark grey)**

## Tables

**Table 1. Primers used for mouse cDNA**

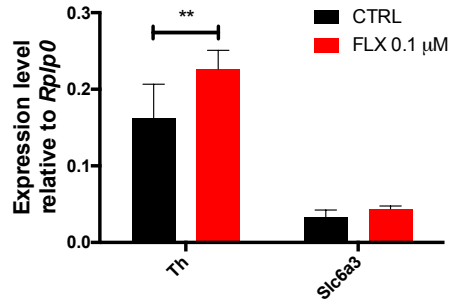
	Forward	Reverse
<i>36B4</i>	GACACCCTCCAGGAAGC	GTGTTCGACAATGGCAG
<i>ER<math>\alpha</math></i>	CTGTCCAGCAGTAACGA	CACAGTAGCGAGTCTCC
<i>ER<math>\beta</math></i>	TGCCTGTAAACAGAGAG	AGTCATTATGTCCTTGA
<i>Tubb3</i>	TGTCATCCACCTTCATT	AACATGGCTGTGAACTG
<i>Nes</i>	AGGGCAAATCTGGGAA	AGGGTTTCCATCTGCAA
<i>En1</i>	ACAGAGAAAGCGAGCA	TTTTTCCCCCATAGCAC
<i>En2</i>	AGGTTCCAAGACGCTAT	TTTGAGCACTCCATCCA
<i>Otx2</i>	GTCTTATCTAAAGCAAC	AGTAAATGTCGTCCTCT
<i>Nkx2.2</i>	GTGATCGTTGCCAAATG	TGCTCAGGAGACGAAA
<i>Lmx1a</i>	AGCGAGCCAAGATGAA	TTGTCTGAGCAGAAGTC
<i>Pitx3</i>	ACGGCTCTCTGAAGAAG	CATGTCAGGGTAGCGAT
<i>Th</i>	ATTGGAGGCTGTGGTAT	ACTTTCAAAGCCCGAGA
<i>Slc6a3</i>	ATGTCTTCACACTGCTG	ATTGCTGGACACCGTAG
<i>Tph2</i>	GTGACCCTGAATCCGCC	GGTGCCGTACATGAGG
<i>Slc6a4</i>	GTTGATGCTGCGGCTCA	GAAGCTCGTCATGCAGT
<i>Foxp2</i>	AAGGAGCAGTGTGGAC	GCAGACTGGCATTTAGA
<i>Gria2</i>	GCCGAGGCGAAACGAA	CACTCTCGATGCCATAT
<i>Pax3</i>	CCGGGGCAGAATTACCC	GCCGTTGATAAATACTC
<i>Rora</i>	GTGGAGACAAATCGTCA	TGGTCCGATCAATCAAA
<i>Reln</i>	TTACTCGCACCTTGCTG	CAGTTGCTGGTAGGAGT



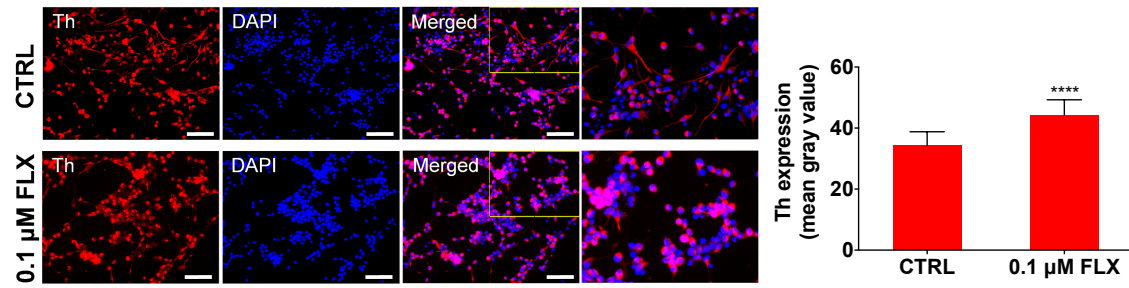
Figure 1

A

Molecular Pharmacology Fast Forward. Published on August 16, 2018 as DOI: 10.1124/mol.118.112342  
This article has not been copyedited and formatted. The final version may differ from this version.



B



C

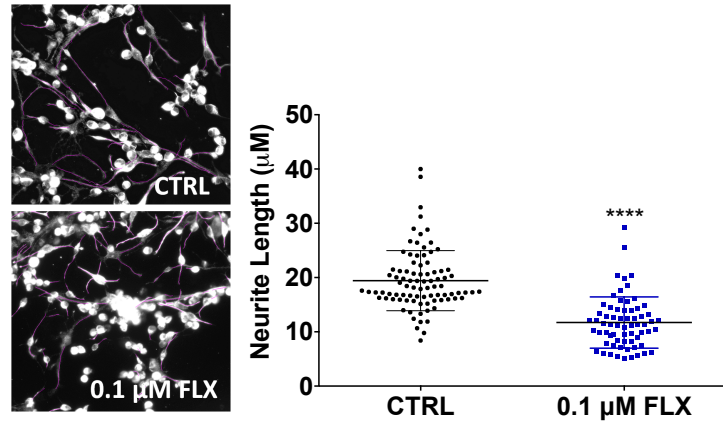
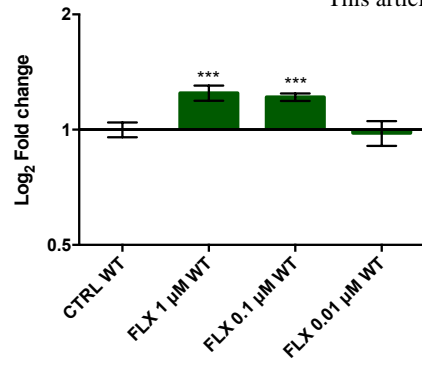


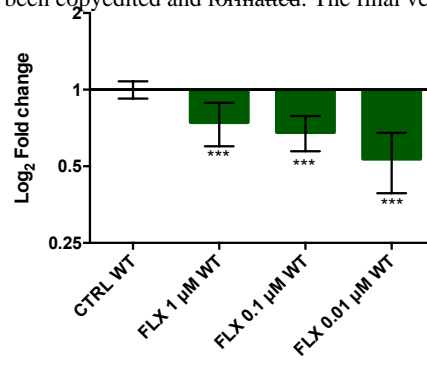
**Figure 2**

*Otx2*

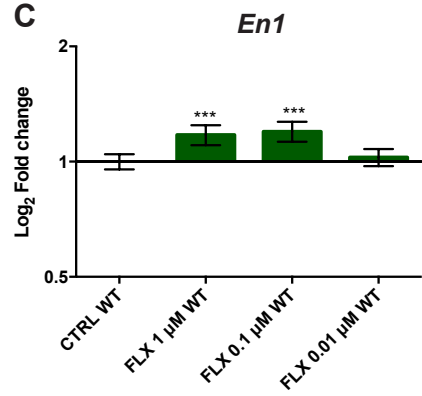
**A**



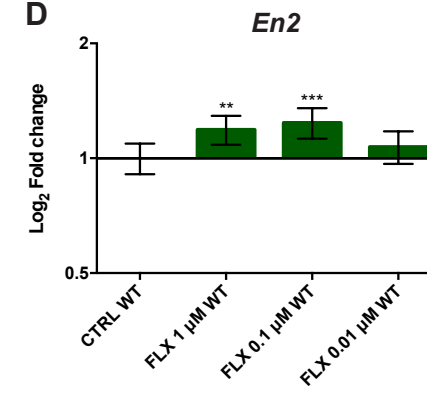
**B**



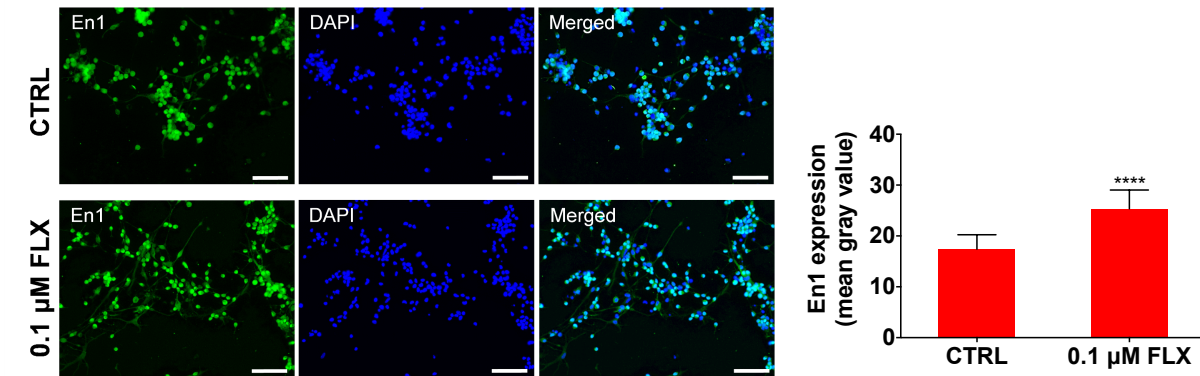
**C**



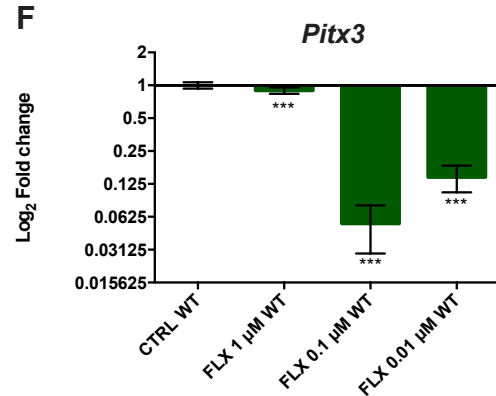
**D**



**E**



**F**



**G**

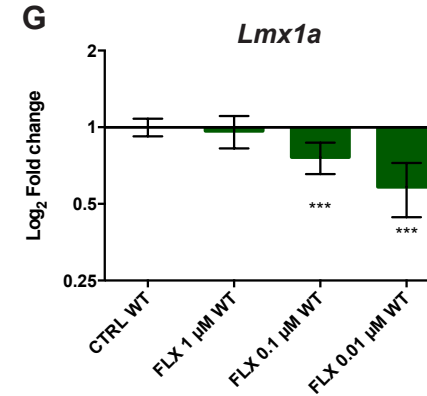


**Figure 3**

Molecular Pharmacology Fast Forward. Published on August 16, 2018 as DOI: 10.1124/mol.118.112342  
This article has not been copyedited and formatted. The final version may differ from this version.

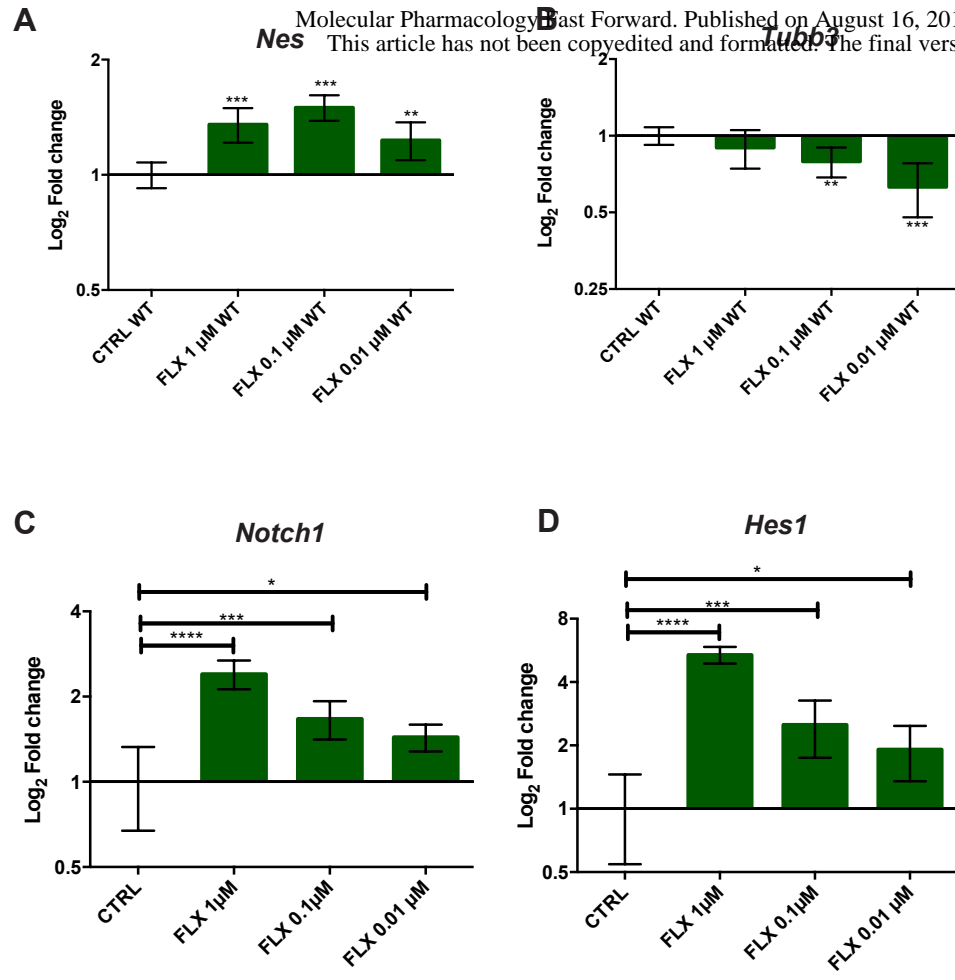
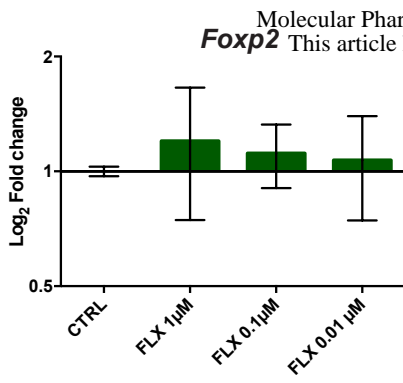
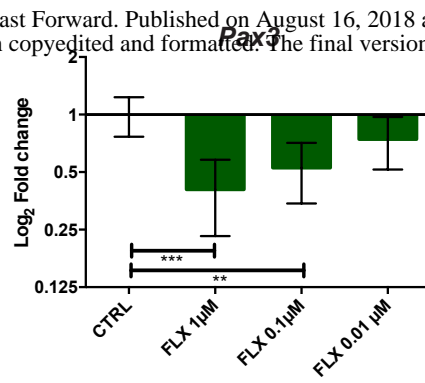


**Figure 4**

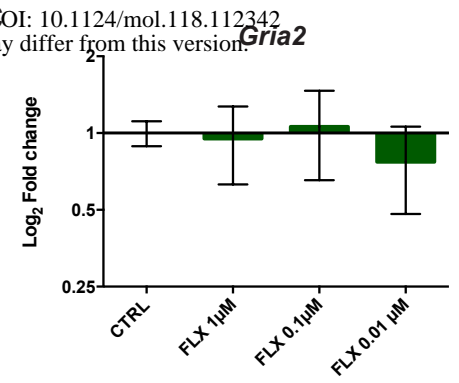
**A**



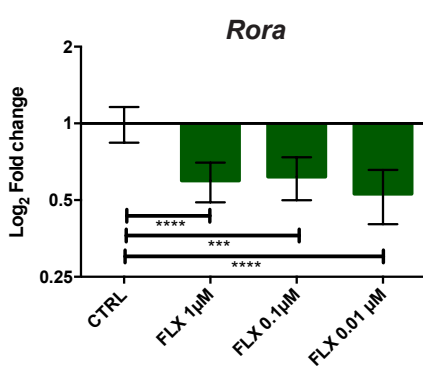
**B**



**C**



**D**



**E**

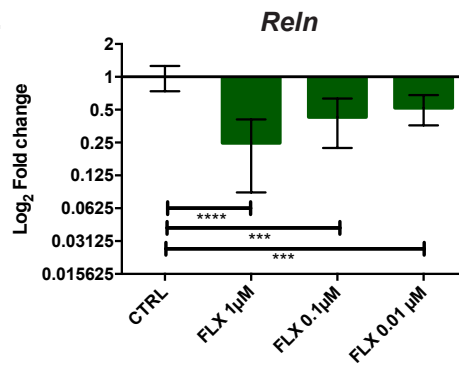


Figure 5

Molecular Pharmacology Fast Forward. Published on August 16, 2018 as DOI: 10.1124/mol.118.112342  
This article has not been copyedited and formatted. The final version may differ from this version.

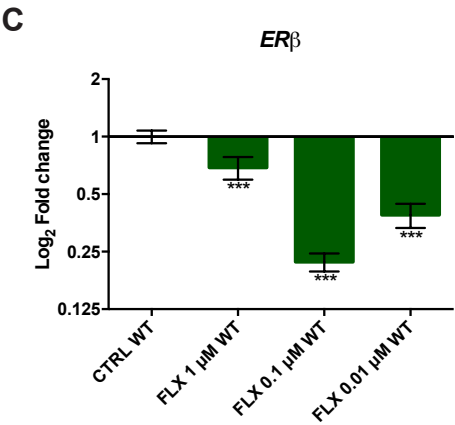
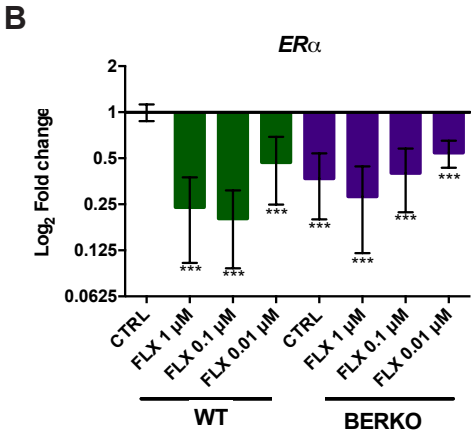
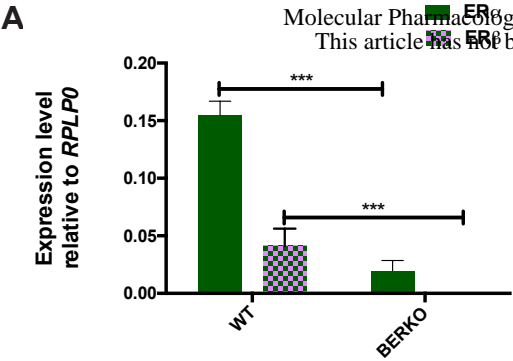
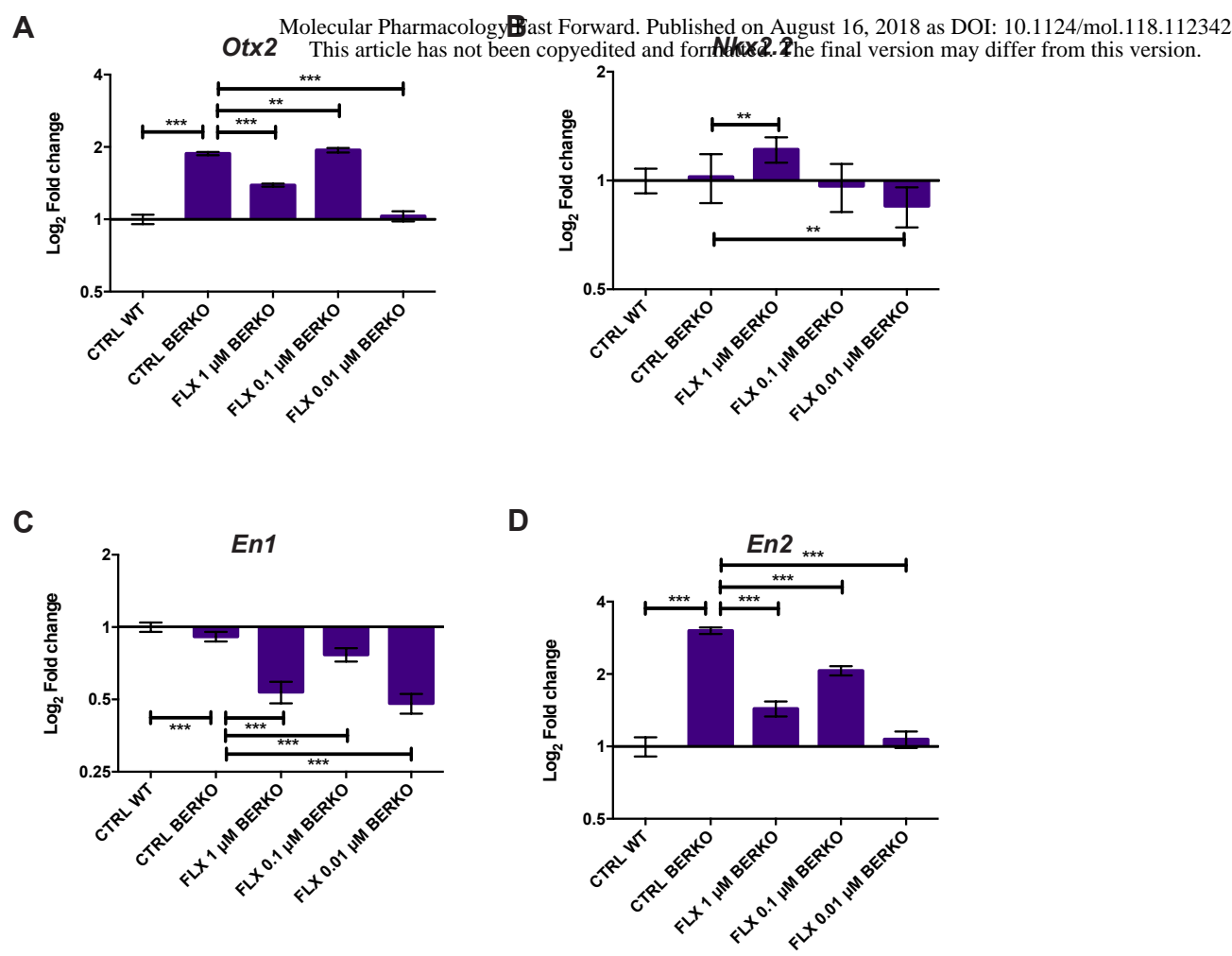


Figure 6



**Figure 7**

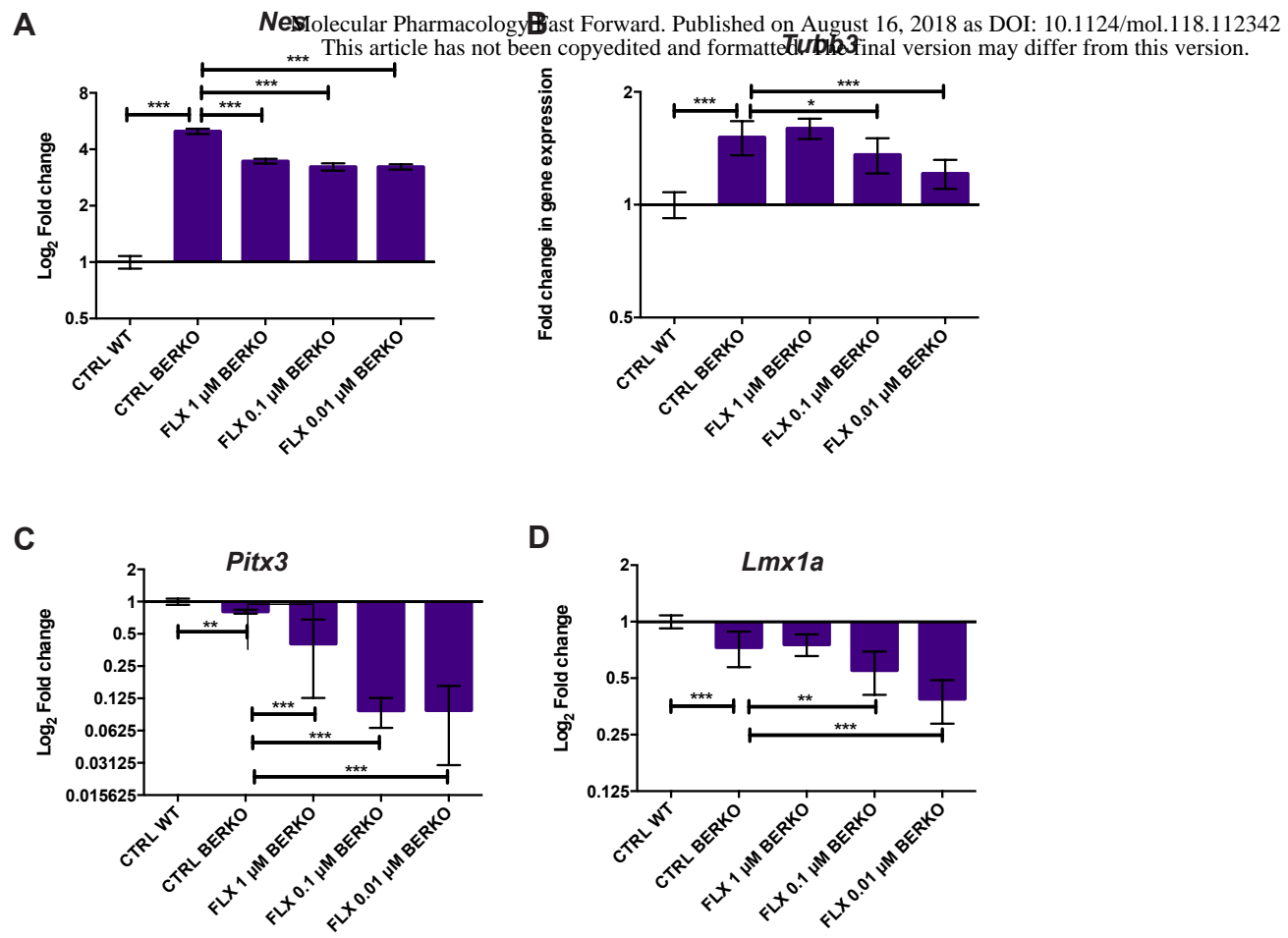
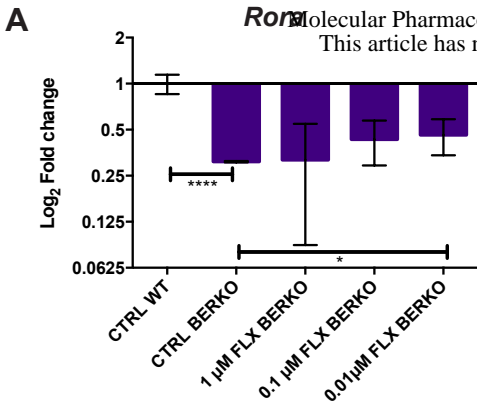


Figure 8

*Rora*

Molecular Pharmacology Fast Forward. Published on August 16, 2018 as DOI: 10.1124/mol.118.112342  
This article has not been copyedited and formatted. The final version may differ from this version.



*Reln*

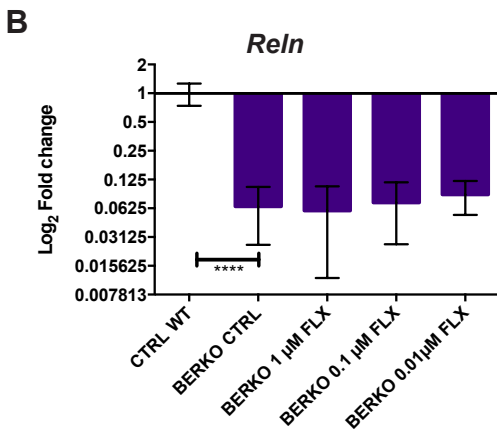
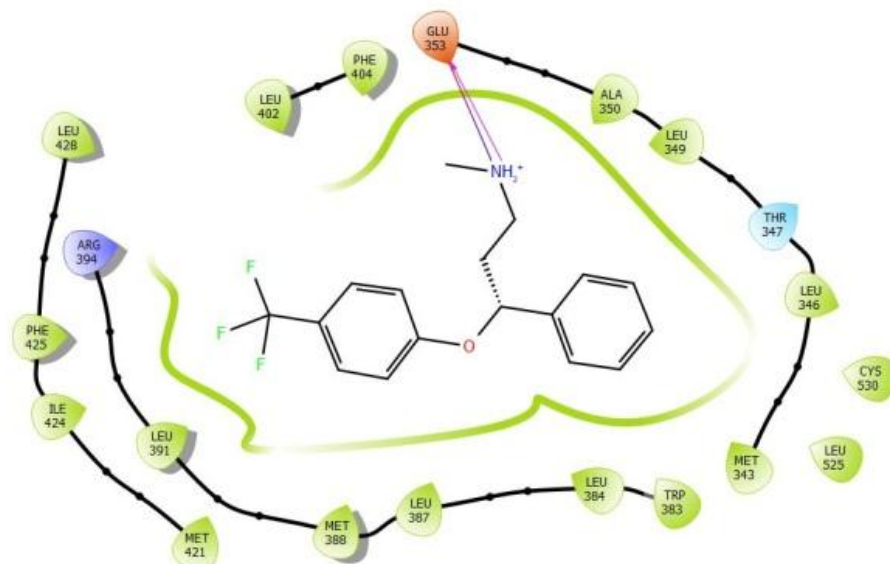




# Figure 9

**A**



**B**

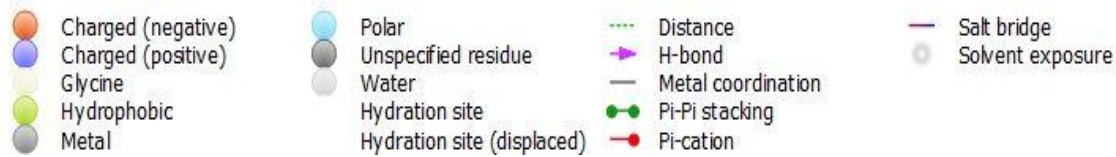
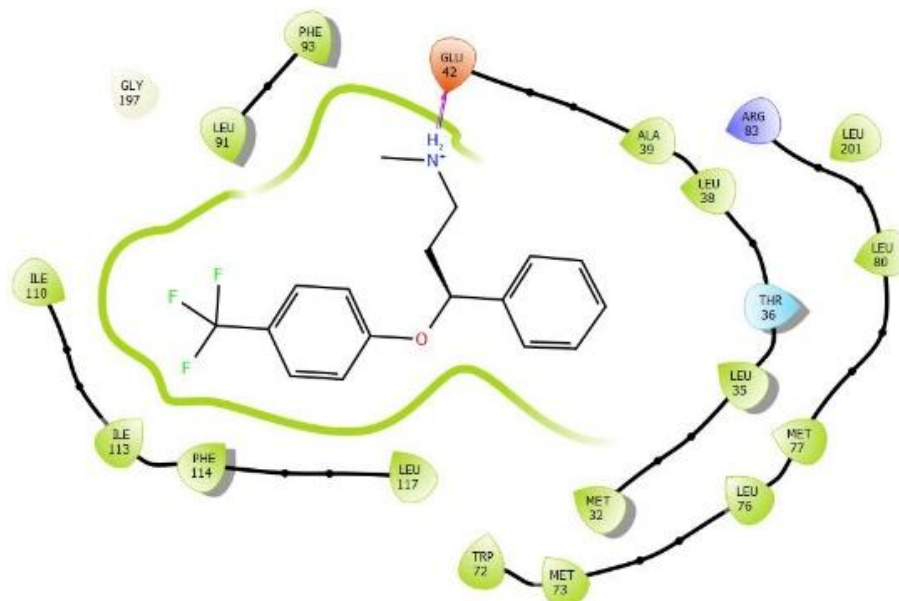
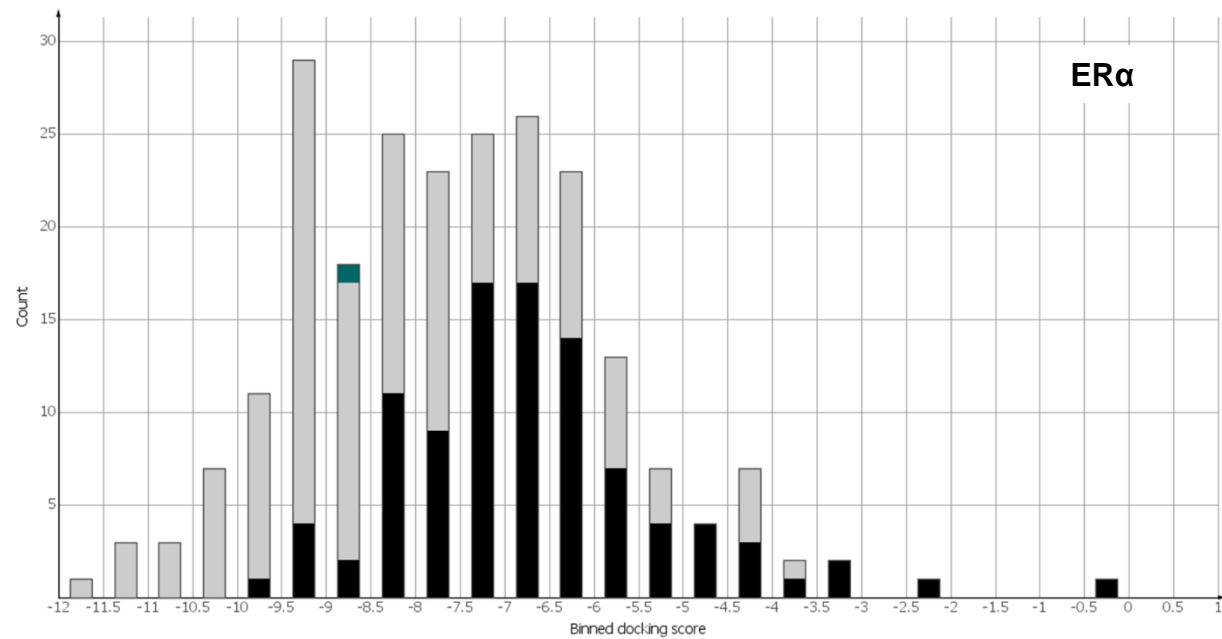


## Figure 10

**A**



**B**

